Dalton
Transactions

ROYAL SOCIETY
OF CHEMISTRY

COMMUNICATION

View Article Online
View Journal | View Issue

Check for updates

Cite this: *Dalton Trans.*, 2025, **54**, 16673

Received 13th October 2025,
Accepted 28th October 2025

DOI: 10.1039/d5dt02464a

rsc.li/dalton

Single-crystal to single-crystal synthesis of a gold(I)-ammonia complex and H/D exchange *in crystallo* with D_2O

Chloe L. Johnson, [a] Kristof M. Altus, [a] Miquel Navarro, [b] Jesús Campos, [b] Simon B. Duckett *[a] and Andrew S. Weller *[a]

Single-crystal to single-crystal solid/gas reactivity of [LAu(C_2H_4/CO)][$BAr^F{}_4$] [L = tris-2-(4,4′-di-*tert*-butylbiphenyl)phosphine] with NH_3 or $^{15}NH_3$ gives the ammonia complexes [LAu(NH_3/$^{15}NH_3$)][$BAr^F{}_4$]. Solid–gas H/D exchange with D_2O vapour gives the ND_3 isotopologues, while reaction with HCl vapour affords [1-Cl]/[$^{15}NH_4$][$BAr^F{}_4$], identifying a lattice encapsulated ammonium as a plausible intermediate species for H/D exchange with D_2O by a proton rebound mechanism.

Solid-state molecular organometallic chemistry (SMOM[1]) offers new opportunities for synthesis and catalysis using single-crystal to single-crystal (SC-SC) solid–gas reactivity *in crystallo*.[2,3] This approach combines the precise reactivity of well-defined, site-isolated, molecular species with the additional advantages of stability and selectivity that the extended tertiary microenvironment provides through non-covalent secondary interactions.[4] Examples of SMOM include the generation of room-temperature-stable rhodium σ-alkane complexes,[5] reversible methane C–H activation at an Ir-centre,[6] reversible binding of ethene at Ag(I) centres[7] and CO_2 activation at Cu(I) hydrides.[8] We recently reported the synthesis of the Au(I) π-acetylene complex, [LAu(η^2-HC≡CH)][$BAr^F{}_4$] **[1-C_2H_2][$BAr^F{}_4$]**, using the cavity-shaped phosphine [L = tris-2-(4,4′-di-*tert*-butylbiphenyl)phosphine, Ar^F = 3,5-$C_6H_3(CF_3)_2$], by addition of acetylene gas to precursor ethene **[1-C_2H_4][$BAr^F{}_4$]**, or CO containing **[1-CO][$BAr^F{}_4$]**, complexes.[9]

We now reveal that a rare[10] example of a crystallographically characterised Au(I)–ammonia complex (and its ^{15}N isotopologue) can be prepared using such SC–SC routes, and that these complexes undergo complete H/D exchange at NH_3 using D_2O vapour in the solid-state. A mechanism invoking lattice encapsulated $[NH_4]^+$ is proposed, supported by SC–SC reactivity studies using HCl vapour. $[LAu(I)NH_3]^+$ complexes are of interest for their role in olefin hydroamination catalysis;[10–12] while SC–SC reactivity of Au(I) complexes with external stimuli has applications in photoluminescence.[13,14] H/D exchange at bound ammonia is known,[15–19] as are SC–SC organometallic reactions using NH_3.[19,20]

The starting materials **[1-ligand][$BAr^F{}_4$]** (ligand = C_2H_4, CO) crystallise as colourless blocks in two distinct polymorphs that are discriminated by residual solvent in the lattice ($P2_1/n$, 1,2-$F_2C_6H_4$; $P\bar{1}$, 1,2-$F_2C_6H_4$ and heptane).[9] In both, the $[BAr^F{}_4]^-$ anions form a bicapped square prismatic arrangement, in which two crystallographically identical cations of $\mathbf{[1]^+}$ are enclosed by 10 anions (see Supporting Information, SI). While these polymorphs could not be mechanically separated, they dissolve to form a single product in solution (^1H NMR spectroscopy, CD_2Cl_2), before and after SC–SC reactivity. These polymorphs are thus holistically treated as an ensemble.

Addition of NH_3 (1 bar absolute, 10 min) to the bulk ensemble of crystalline **[1-C_2H_4][$BAr^F{}_4$]** results in complete conversion to **[1-NH_3][$BAr^F{}_4$]**, Scheme 1, as measured by single-crystal X-ray diffraction, powder X-ray diffraction, and solution NMR spectroscopy (see SI). Ethene is observed to be formed by gas phase ^1H NMR spectroscopy. In the ^1H NMR spectrum (CD_2Cl_2) the NH_3 ligand is observed as a broad peak at δ 0.92 (fwhm = ~9 Hz). This is significantly upfield-shifted when

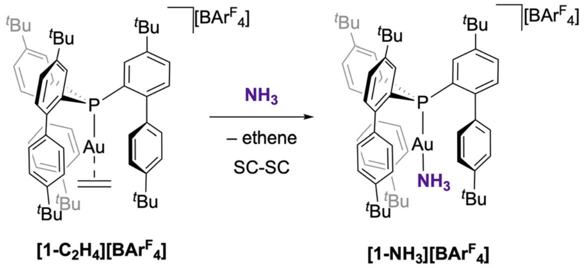

Scheme 1 Synthesis of **[1-NH_3][$BAr^F{}_4$]**.

---

[a] *Department of Chemistry, University of York, Heslington, York, YO10 5DD, UK. E-mail: andrew.weller@york.ac.uk, simon.duckett@york.ac.uk*

[b] *Instituto de Investigaciones Químicas (IIQ), Departamento de Química Inorgánica and Centro de Innovación en Química Avanzada (ORFEO–CINQA) Consejo Superior de Investigaciones Científicas (CSIC) and University of Sevilla, 41092 Sevilla, Spain. E-mail: jesus.campos@iiq.csic.es*

compared with other Au(I)–NH$_3$ complexes, *e.g.* [(CAAC)Au(NH$_3$)][B(C$_6$F$_5$)$_4$] (CAAC = cylicalkylaminocarbene, δ 2.53)[10] and [(PPh$_3$)Au(NH$_3$)][ClO$_4$] (δ 3.85),[21] which we suggest is due to ring current effects of the cavity-shaped aryl phosphine ligand,[11] through proximal N–H/π interactions.[22]

The resulting single-crystal structure of **[1-NH$_3$][BAr$^F_4$]** ($P\bar{1}$ polymorph) shows that the cation has a linear geometry [P–Au–N 177.9(3)°], Fig. 1. The Au–N distance of 2.139(8) Å, is slightly longer than that of the only other crystallographically characterised gold(I) ammonia complex, [(CAAC)Au(NH$_3$)][B(C$_6$F$_5$)$_4$] [2.094(7) Å].[10] The [BAr$^F_4$]$^-$ anions retain the bicapped square prismatic arrangement, however the lattice solvents of **[1-NH$_3$][BAr$^F_4$]** are absent to the detection limit of the X-ray experiment, being lost in this SC–SC reaction as confirmed by ^{1}H NMR spectroscopy on the dissolved ensemble of crystalline materials. The ^{31}P{^{1}H} SSNMR of the ^{15}NH$_3$ analogue (see below) shows a broad, asymmetric peak at δ 3.9, suggestive of the retention of two different crystalline phases in the ensemble.

$$[\mathbf{1\text{-}NH_3}][\mathbf{BAr^F{}_4}] \underset{\substack{H_2O\\ SC-SC}}{\overset{D_2O}{\rightleftharpoons}} [\mathbf{1\text{-}ND_3}][\mathbf{BAr^F{}_4}] \tag{1}$$

This ensemble of crystals of **[1-NH$_3$][BAr$^F_4$]** undergo reversible, and selective, H/D exchange at the bound NH$_3$ ligand in a SC–SC reaction (eqn (1)) upon exposure to an excess of D$_2$O vapour over 1 h, that forms **[1-ND$_3$][BAr$^F_4$]** (see SI for experimental set up). While single-crystal X-ray diffraction shows an unchanged structure, in the ^{1}H NMR spectrum (CD$_2$Cl$_2$) the NH$_3$ peak at δ 0.92 is absent, replaced by an, isotopically-shifted, ND$_3$ peak at δ 0.81 in the ^{2}H NMR spectrum. Upon exposure of crystals of **[1-ND$_3$][BAr$^F_4$]** to moist air, the NH$_3$ peak reappears in the ^{1}H NMR spectrum (CD$_2$Cl$_2$), indicating that this process is reversible and facile. ESI-MS (Electrospray Ionisation Mass Spectrometry, positive mode, CH$_2$Cl$_2$) of **[1-ND$_3$][BAr$^F_4$]** only returns an isotopologue pattern consistent with **[1-NH$_3$][BAr$^F_4$]**, likely due to exposure of the complex to trace moisture in the sample train, despite significant precautions being taken.[23] Likewise, the solid-state ATR-IR spectrum of crystals of **[1-ND$_3$][BAr$^F_4$]** measured in air matches that of **[1-NH$_3$][BAr$^F_4$]** [$\nu_{(N-H)}$ = 3359 cm^{-1}], with this vibration absent when measured in an argon-filled glove box.[24] Using commercially sourced D$_2$ (99.96%) H/D exchange is also observed to give **[1-ND$_3$][BAr$^F_4$]**. However, when dried D$_2$ was used (1 week over 3 Å molecular sieves) no exchange occurred. We thus suggest trace D$_2$O is the source of deuterium under these conditions. **[1-ND$_3$][BAr$^F_4$]** can be independently prepared in a SC–SC transformation by exposure of the ensemble of crystalline **[1-C$_2$H$_4$][BAr$^F_4$]** to ND$_3$ (SI).

To discount the formation of the isoelectronic water complex on addition of H$_2$O, *i.e.* **[1-OH$_2$][BAr$^F_4$]**, H/D exchange studies were repeated using the ^{15}N labelled isotopologue **[1-^{15}NH$_3$][BAr$^F_4$]**. This was synthesised by addition of ^{15}NH$_3$ (~0.5 bar) to crystals of the ensemble of polymorphs of **[1-CO][BAr$^F_4$]** that resulted in 94% conversion (^{31}P{^{1}H} NMR, CD$_2$Cl$_2$) to **[1-^{15}NH$_3$][BAr$^F_4$]**, Fig. 2A.[25] In the resulting ^{15}N NMR spectrum of **[1-^{15}NH$_3$][BAr$^F_4$]** (CD$_2$Cl$_2$, Fig. 2B) a quartet of doublets is observed [δ 6.2, $^1J_{NH}$ = 72 Hz, $^2J_{NP}$ = 38 Hz], which collapses into a doublet [$^2J_{NP}$ = 38 Hz] on ^{1}H decoupling. The ^{15}NH$_3$ signal is observed as a doublet at δ 0.90 [$^1J_{HN}$ = 72 Hz] in the ^{1}H NMR spectrum, Fig. 2C. The ^{31}P{^{1}H} NMR spectrum shows coupling to ^{15}N [δ 3.6, $^2J_{NP}$ = 38 Hz]. Solid-state ^{31}P{^{1}H} and ^{15}N{^{1}H} NMR spectra are fully consistent with the formulation (SI). Addition of D$_2$O to crystalline **[1-^{15}NH$_3$][BAr$^F_4$]** resulted in the disappearance of the ^{15}NH$_3$ peak in the resulting ^{1}H NMR spectrum (CD$_2$Cl$_2$) and the appearance of a peak corresponding to H$_2$O at δ 1.56, Fig. 2D. Retention of bound ammonia in the complex is confirmed by the observation of ^{15}ND$_3$ as a doublet in the ^{2}H NMR spectrum at δ 0.84 [$^1J_{DN}$ = 9 Hz]. Rapid proton exchange between H$_2$O and bound NH$_3$ was demonstrated by solution EXSY experiments (CD$_2$Cl$_2$, 298 K); calculated to be 13.8 ± 0.4 s^{-1}, that corresponds to a barrier of 15.9(2) kcal mol^{-1}.

H/D exchange at Rh(I)-bound NH$_3$ has been reported previously in the solid-state using D$_2$, and is proposed to operate *via* formation of an outer sphere ammonium complex.[19]

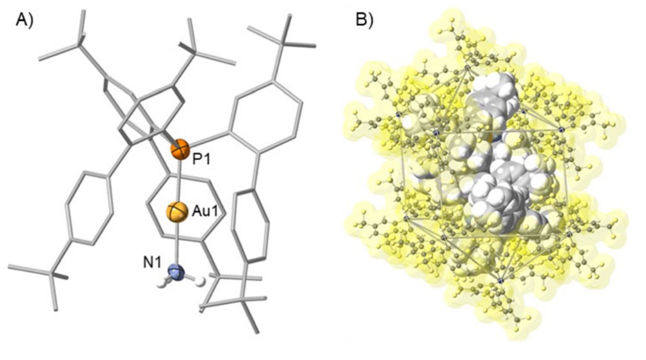

Fig. 1 (A) Molecular structure of the cation **[1-NH$_3$]$^+$** ($P\bar{1}$ polymorph). Displacement ellipsoids shown at 50% probability. Most hydrogen atoms are excluded for clarity. Selected bond distances (Å) **[1-NH$_3$][BAr$^F_4$]**, Au–N, 2.139(8); Au–P, 2.234(3). (B) Packing diagram of **[1-NH$_3$][BAr$^F_4$]** shown at van der Waals radii.

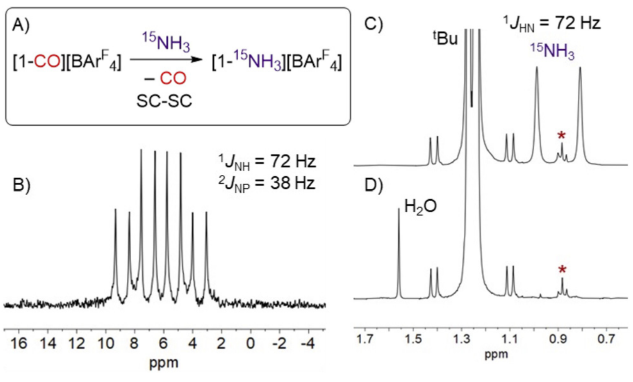

Fig. 2 (A) Synthesis of **[1-^{15}NH$_3$][BAr$^F_4$]**. (B) ^{15}N NMR spectrum. (C) NH$_3$ region of the ^{1}H NMR spectrum. (D) ^{1}H NMR spectrum after D$_2$O addition to single-crystals (all 500 MHz, CD$_2$Cl$_2$, 298 K). * Residual heptane.

Similarly, one possible mechanism of H/D exchange at the Au(I)-bound NH_3 with D_2O is *via* protonolysis by lattice-incorporated D_2O[26] to form an $[NH_3D]^+$ cation and a neutral LAu(I)–OD complex, Scheme 2. A proton rebound mechanism then delivers the isotopically-enriched ammonia complex, and HDO, Scheme 2. Au(I) hydroxide complexes, including **[1-OH]**, are known,[27–29] and protonation with acids has been shown to eliminate water.

An alternative, closely-related, mechanism is deprotonation of the bound NH_3 by lattice proximal D_2O to form a neutral amido intermediate and $[D_2HO]^+$ [15,16] that rapidly undergoes a rebound mechanism to deliver $[LAu–NH_2D][BAr^F_4]$/HDO.

To demonstrate the feasibility of a rebound mechanism occurring in the lattice, the ensemble of crystalline **$[1\text{-}^{15}NH_3][BAr^F_4]$** was exposed to HCl vapour for 30 days.[30] This resulted in ∼90% conversion to **$[1\text{-Cl}]/[^{15}NH_4][BAr^F_4]$**. A resulting single-crystal X-ray structure ($P2_1/n$), Fig. 3, reveals an ammonium cation (0.9 occupancy, confirmed by solution $^{31}P\{^1H\}$ NMR spectroscopy) residing within a pocket created by the phosphine ligand, accommodated by a twist of one of the phosphine biaryl substituents. In the $^{15}N\{^1H\}$ SSNMR spectrum of the crystalline product two sharp signals observed at δ 39.9 and 31.1 are assigned to the crystallographically-distinct $[^{15}NH_4]^+$ cations of the two different polymorphs. In the solution ^1H NMR (CD_2Cl_2) spectrum the $[^{15}NH_4]^+$ cation was observed as a doublet at δ 5.57 [$^1J_{HN}$ = 74 Hz], which collapses to a singlet upon $\{^{15}N\}$ decoupling, with a $^1H–^{15}N$ HMBC correlation to a ^{15}N signal at δ 33.8.

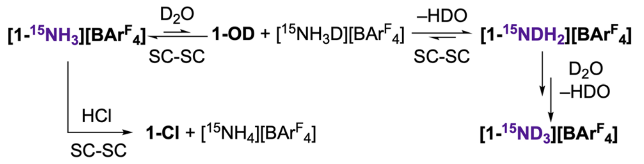

Scheme 2 Reaction of **$[1\text{-}^{15}NH_3][BAr^F_4]$** with D_2O and HCl and postulated intermediates.

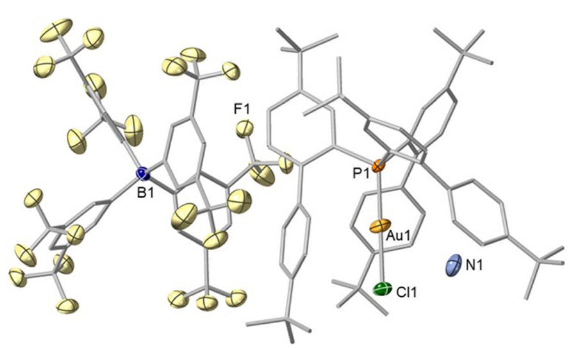

Fig. 3 Molecular structure of the SC–SC reaction of complex **$[1\text{-}^{15}NH_3][BAr^F_4]$** with HCl after 30 days. Displacement ellipsoids are set at 50% probability level. Hydrogen atoms are excluded for clarity. Selected bond distances (Å): Au1–Cl1, 2.325(3); Au1–P1, 2.231(2). Selected bond angles (°): N1–Au1–P1, 176.59(9).

In conclusion, by extending the SMOM methodology to the synthesis and reactivity of Au(I)–NH_3 complexes the broader applicability of the approach is demonstrated, allowing for the synthesis of a range isotopologues (^2H, ^{15}N) and mechanistic insight into H/D exchange *in crystallo*. Our observations also suggest a plausible source of deuterium in commercial D_2 is, in fact, D_2O, and thus its presence needs to be considered in mechanistic studies using as supplied D_2.

Author contributions

CLJ, KA and MN carried out the experimental work. CLJ wrote the first draft of the manuscript. JC, SBD and ASW directed the research. All authors contributed to the final manuscript.

Conflicts of interest

There are no conflicts to declare.

Data availability

The data supporting this article have been included as part of the supplementary information (SI). Supplementary information is available. See DOI: https://doi.org/10.1039/d5dt02464a.

CCDC 2493494 (**$[1\text{-}NH_3][BAr^F_4]$**) and 2493496 (**$[1\text{-Cl}]/[^{15}NH_4][BAr^F_4]$**) contain the supplementary crystallographic data for this paper.[31a,b]

Acknowledgements

The Leverhulme Trust (RPG-2020-184), EPSRC (EP/W015552/1) and the Wild Overseas Scholar's Fund. M. N. acknowledges the Junta de Andalucía for postdoctoral program (DOC_00149). MCIU/AEI/10.13039/501100011033 (PID2022-139782NB-I00). Marc Reid (Strathclyde), Guy Lloyd-Jones (Edinburgh) and John Hartwig (Berkley) are thanked for useful discussions.

References

1 F. M. Chadwick, A. I. McKay, A. J. Martinez-Martinez, N. H. Rees, T. Krämer, S. A. Macgregor and A. S. Weller, *Chem. Sci.*, 2017, **8**, 6014–6029.
2 K. A. Reid and D. C. Powers, *Chem. Commun.*, 2021, **57**, 4993–5003.
3 A. Sur and D. C. Powers, *ACS Cent. Sci.*, 2025, **11**, 834–842.
4 M. A. Sajjad, S. A. Macgregor and A. S. Weller, *Faraday Discuss.*, 2023, **244**, 222–240.
5 A. J. Bukvic, A. L. Burnage, G. J. Tizzard, A. J. Martínez-Martínez, A. I. McKay, N. H. Rees, B. E. Tegner, T. Krämer, H. Fish, M. R. Warren, S. J. Coles, S. A. Macgregor and A. S. Weller, *J. Am. Chem. Soc.*, 2021, **143**, 5106–5120.

6 M. R. Gyton, M. A. Sajjad, D. J. Storm, K. M. Altus, J. C. Goodall, C. L. Johnson, S. J. Page, A. J. Edwards, R. O. Piltz, S. B. Duckett, S. A. Macgregor and A. S. Weller, *J. Am. Chem. Soc.*, 2025, **147**, 8706–8719.

7 H. V. R. Dias, D. Parasar, A. A. Yakovenko, P. W. Stephens, Á. Muñoz-Castro, M. Vanga, P. Mykhailiuk and E. Slobodyanyuk, *Chem. Sci.*, 2024, **15**, 2019–2025.

8 E. A. Patrick, M. E. Bowden, J. D. Erickson, R. M. Bullock and B. L. Tran, *Angew. Chem., Int. Ed.*, 2023, **62**, e202304648.

9 C. L. Johnson, D. J. Storm, M. A. Sajjad, M. R. Gyton, S. B. Duckett, S. A. Macgregor, A. S. Weller, M. Navarro and J. Campos, *Angew. Chem., Int. Ed.*, 2024, **63**, e202404264.

10 V. Lavallo, G. D. Frey, B. Donnadieu, M. Soleilhavoup and G. Bertrand, *Angew. Chem., Int. Ed.*, 2008, **47**, 5224–5228.

11 M. Navarro, M. G. Alférez, M. de Sousa, J. Miranda-Pizarro and J. Campos, *ACS Catal.*, 2022, **12**, 4227–4241.

12 G. Kovács, A. Lledós and G. Ujaque, *Angew. Chem., Int. Ed.*, 2011, **50**, 11147–11151.

13 S. H. Lim, M. M. Olmstead and A. L. Balch, *Chem. Sci.*, 2013, **4**, 311–318.

14 M.-S. Jiang, Y.-H. Tao, Y.-W. Wang, C. Lu, D. J. Young, J.-P. Lang and Z.-G. Ren, *Inorg. Chem.*, 2020, **59**, 3072–3078.

15 G. L. Hillhouse and J. E. Bercaw, *J. Am. Chem. Soc.*, 1984, **106**, 5472–5478.

16 R. Koelliker and D. Milstein, *J. Am. Chem. Soc.*, 1991, **113**, 8524–8525.

17 A.-K. Jungton, P. Kläring, T. Braun and A. Eißler, *Z. Anorg. Allg. Chem.*, 2012, **638**, 505–511.

18 A.-K. Jungton, C. Herwig, T. Braun and C. Limberg, *Chem. – Eur. J.*, 2012, **18**, 10009–10013.

19 S. D. Pike, T. Krämer, N. H. Rees, S. A. Macgregor and A. S. Weller, *Organometallics*, 2015, **34**, 1487–1497.

20 Z. Huang, P. S. White and M. Brookhart, *Nature*, 2010, **465**, 598–601.

21 J. Vicente, M.-T. Chicote, R. Guerrero, P. G. Jones and M. C. R. D. Arellano, *Inorg. Chem.*, 1997, **36**, 4438–4443.

22 J. P. Blagojević Filipović, D. Z. Vojislavljević-Vasilev and S. D. Zarić, *Cryst. Growth Des.*, 2024, **24**, 1705–1714.

23 A. T. Lubben, J. S. McIndoe and A. S. Weller, *Organometallics*, 2008, **27**, 3303–3306.

24 The isotopically-shifted N–D stretch at 2453 cm^{-1} (calc) was not observed. Nevertheless all other data support the formation of ND_3.

25 Incomplete conversion is likely due to the lower pressure used. We discount an equilbrium as addition of CO to **[1-NH$_3$][BArF$_4$]** resulted in no observable reaction.

26 I. J. Vitórica-Yrezábal, G. Mínguez Espallargas, J. Soleimannejad, A. J. Florence, A. J. Fletcher and L. Brammer, *Chem. Sci.*, 2013, **4**, 696–708.

27 S. Gaillard, A. M. Z. Slawin and S. P. Nolan, *Chem. Commun.*, 2010, **46**, 2742–2744.

28 M. Navarro, M. Holzapfel and J. Campos, *Inorg. Chem.*, 2023, **62**, 10582–10591.

29 S. R. Patrick, A. Gómez-Suárez, A. M. Z. Slawin and S. P. Nolan, *Organometallics*, 2013, **33**, 421–424.

30 G. Mínguez Espallargas, J. van de Streek, P. Fernandes, A. J. Florence, M. Brunelli, K. Shankland and L. Brammer, *Angew. Chem., Int. Ed.*, 2010, **49**, 8892–8896.

31 (*a*) CCDC 2493494: Experimental Crystal Structure Determination, 2025, DOI: 10.5517/ccdc.csd.cc2ppp9d; (*b*) CCDC 2493496: Experimental Crystal Structure Determination, 2025, DOI: 10.5517/ccdc.csd.cc2pppcg.